Low Discrepancy Holographic Image Sampling

Alfred M. Bruckstein,[1] Robert J. Holt,[2] Arun N. Netravali[2]

[1] Department of Computer Science, Technion, Israel Institute of Technology, Haifa 32000, Israel

[2] Bell Laboratories, Lucent Technologies, Murray Hill, NJ 07974, USA

Received 30 September 2004; revised 10 April 2005; accepted 20 April 2005

ABSTRACT: Self-similar progressive image sampling schemes that have been recently proposed for holographic image representations are shown to generate two-dimensional low discrepancy sequences. The discrepancy of a planar set of points is a measure of the uniformity of their placement in the plane. Sequences, or planar sets of points with low discrepancy, cover the image domain as uniformly as possible. Int J Imaging Syst Technol, 15, 155–167, 2005; Published online in Wiley InterScience (www.interscience.wiley.com). DOI 10.1002/ima.20051

Key words: discrepancy; image sampling; pixel sequences; uniform coverage

I. INTRODUCTION

Images are bivariate functions, or in the discrete setting, two-dimensional arrays of values. Images must often be moved from one place to another via channels that only allow sequential transmission and hence, we need to map them into one-dimensional strings of numbers. The straightforward way to achieve this is to sample the image at various locations and send these samples one after the other. Several types of image sampling strategies have been invented. Each of these was adapted to special technical requirements. The common sampling and transmission strategy is the raster scan: it is a line-by-line ordered scanning of the image and has the advantage of being simple, systematic, and adapted to the way images are read out from CCD sensing devices. With this image transmission scheme, the location of each pixel is implicitly coded in time and some synchronization is needed to establish the temporal frames. There are several versions of raster scan that have been implemented: the straightforward, noninterlaced version, the interlaced one, and the forward/backward scan (see Fig. 1).

Other systematic image samplings or image scans have been invented. The space filling curves of Peano and Hilbert are recursively defined and have some good properties in terms of visiting and transmitting pixels that have highly correlated gray levels. This is due to the fact that the space filling curves map most spatially neighboring pixels into neighboring pixels in the one-dimensional sequence generated by the scan. See Gotsman and Lindenbaum (1996) for a nice analysis of the 2D-"metric" properties of space filling scans. As stated above, the aim of such scans is to place pixels that are near in the plane and near in linear sequence too. There are of course limitations on what can be achieved, and for a special case, Mitchison and Durbin (1986) found "optimal scans" that minimize the average absolute distance in the linear sequence of all pixels that are 4-neighbors in the image. See Figure 2 for a space filling scan and an optimal scan in the sense of Mitchison and Durbin (1986).

The systematic scannings/samplings that were discussed so far enable us to encode the pixel location implicitly in timing, and hence require synchronized transmission of the image data or the placement of synchronization/location information at some sparse locations in the one-dimensional strings of pixel values. The ordering of sampling locations involved in these implies that if only a portion of the one-dimensional stream of image data is made available, it will enable the recovery of an image portion with shape and location highly dependent upon the location and size of data available. Images are usually highly redundant, however, and if a sampling process would spatially spread the sample locations evenly in the image plane at each stage of the process of generating the linear stream of data, we could form cropped portions of the data stream recover (distorted) versions of the whole image. The quality of the whole image recovered would gradually improve with the increase in the number of image samples available. Such a sampling schedule that ensures an even spread of image samples for every contiguous portion in the sequential ordering of these samples would hence result in a "holographic" property in terms of image recovery. This is a very desirable property indeed if we want the image transmission process to be robust to losses of arbitrary portions of the data. One way to achieve uniformity in the spatial spread of the samples for every contiguous portion of their sequential ordering is to sample the image plane at random. This method has the great disadvantage of requiring the attachment to each pixel's sampled gray-level and the exact location coordinates too, since there is no systematic way in which the recipient of the stream of samples can properly place them in the image-plane otherwise.

Systematic methods for achieving holographic sampling, with the advantage of only rarely requiring explicit pixel-location (or

Correspondence to: Robert J. Holt, Department of Mathematics and Computer Science, Queensborough, City University of New York, Bayside, NY 11364, USA; e-mail: rjholt@qcc.cuny.edu

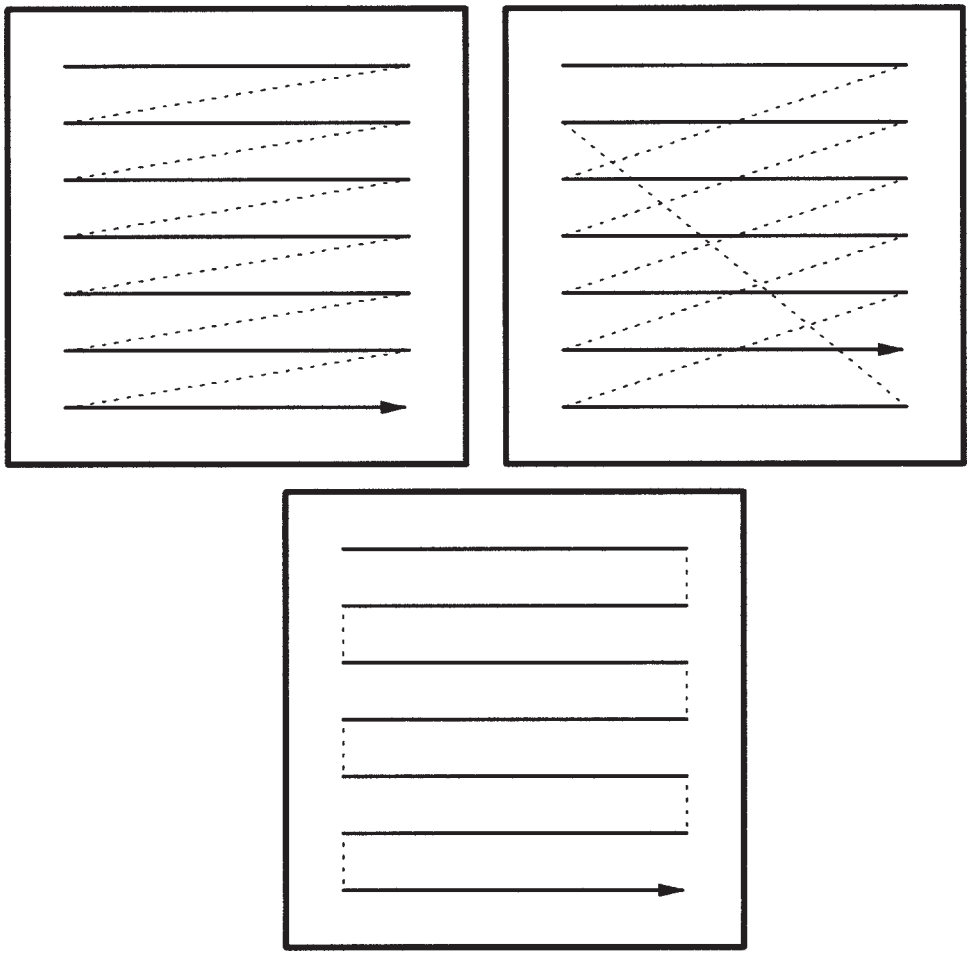

Figure 1. Various types of raster scan.

equivalently, synchronization) information and achieving "uniform" coverage of the image plane for every contiguous portion of the data stream were recently discussed in Bruckstein et al. (1998).

In this paper, we shall show that these holographic image-sampling schemes have good properties in terms of several classical and new measures for assessing the spread or evenness of the sample distributions. In particular, discrepancy has been used to measure the irregularities of distributions of points in space, and in this paper we shall discuss the new sampling schemes in view of discrepancy.

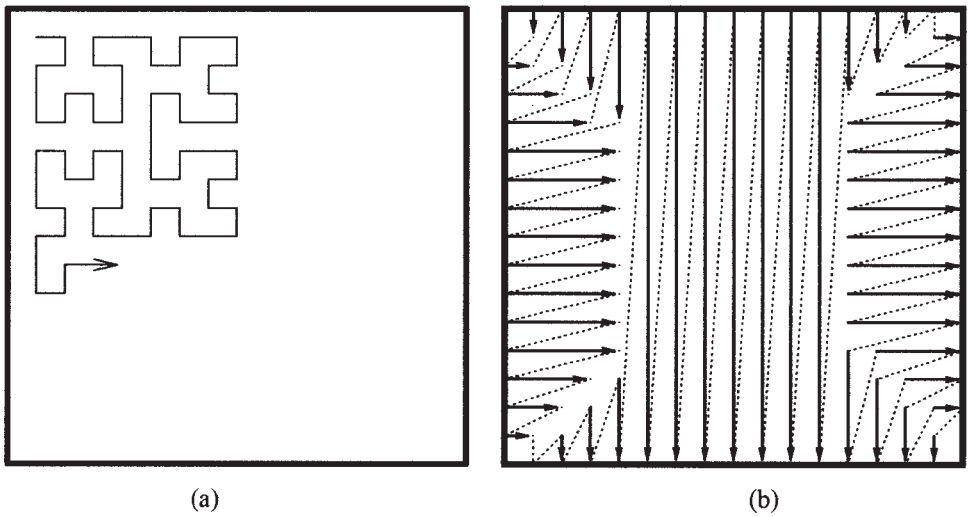

Figure 2. (a) Space filling scan; (b) optimal scan in sense of Mitchison and Durbin (1986) .

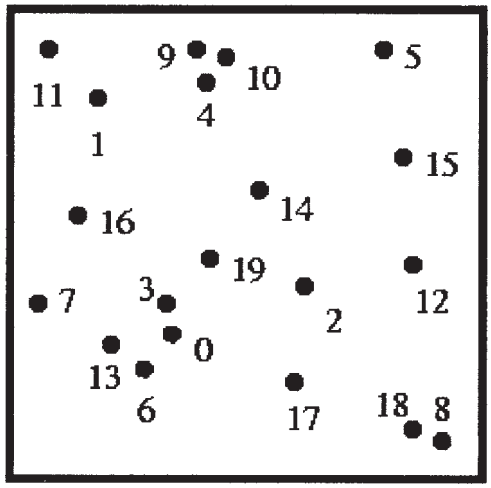

Figure 3. A sequence of random points selected from the unit square.

This paper is organized as follows: Section II next discusses the ways to analyze the spatial distributions of points via discrepancy measures. Then Section III introduces a class of holographic self-similar image sampling processes and their basic properties, and Section IV analyzes the properties of these sampling processes in view of their discrepancies.

II. ANALYSIS BY DISCREPANCY

A. Random Sampling and Its Properties. One of the simplest sampling techniques is to select points at random from the unit square, as in Figure 3. However, simplicity is about the only virtue of this technique. As the distribution tends to a uniform one for a large number of points, or

$$\frac{1}{\text{Total no. of points}} E\{\text{No. of points in region } A\} = \frac{\text{Area}(A)}{\text{Total image area}}, \quad (1)$$

there are usually clumping effects, or clusters of points at each stage. As the placing of random points in a region follows a binomial distribution, a measure of the clumping is given by the variance:

$$\frac{1}{\text{Total no. of points}} \text{Var}\{\text{No. of points in region } A\} = \frac{\text{Area}(A)[\text{Total image area} - \text{Area}(A)]}{(\text{Total image area})^2}.$$

Thus for small regions, the variance is close to the mean (as the binomial distribution approximates a Poisson distribution for a large number of points), which indicates that one can expect a significant amount of clumping. A lack of clumping would lead to a variance near zero.

In addition, with random sampling we need to specify explicitly the location with each value, and this requires the addition of $(2K)$ bits of information to each sample value, where the size of the image is $2^K \times 2^K$.

B. Local Discrepancies of Sequences. To eliminate the need for providing the location for every point, we could use a single pre-specified sequence for any $2^K \times 2^K$ image. To determine whether a sequence is useful, we will need some sort of measure, indicating how well (1) is satisfied throughout the image or unit square. This measure is known as the *discrepancy* of a sequence, and will be discussed now.

Let $\mathbf{x} = (x^{(1)}, \ldots, x^{(d)})$ be points in Euclidean d-space, and $S = (\mathrm{x}_1, \ldots, \mathrm{x}_N)$ be a finite sequence of points in the d-dimensional unit cube $I^d \triangleq 0 \le x^{(i)} < 1, i = 1, \ldots, d$. Next, let χ_J denote the characteristic function of J, where J is a subset of I^d, so that $\sum_{n=1}^{N} \chi_J(\mathbf{x}_n)$ is the number of points of S in J. The *local discrepancy* (Zaremba, 1968; Halton, 1970; Morokoff and Caflisch, 1994) is defined as

$$R_N(J) = \frac{1}{N} \sum_{n=1}^{N} \chi_J(\mathbf{x}_n) - m(J),$$

where $m(J)$ is the volume of J. This is the difference between the actual and expected number of points in the set J, provided that the points come from a uniform random sampling.

An overall discrepancy can now be defined by summing the local discrepancies over various classes of sets θ, and using an arbitrary positive real number m as the norm, as in

$$\left\{ \sum_{J \in \theta} [R_N(J)]^m \right\}^{1/m}.$$

The most popular choices of norm are $m = 2$, yielding a root mean square discrepancy, and $m = \infty$, yielding a supremum, or worst-case, discrepancy. We now look at the most common classes of test areas θ, and one new one that fits in nicely for discretized images.

C. Types of Test Regions. The two classes of test regions that have been used are the class of all rectangular parallelepipeds within the d-dimensional unit cube, and all rectangular parallelepipeds with one corner at the origin. The latter involves easier computations as it involves d parameters compared to the $2d$ of the former, and has received most of the attention in the literature. Formally, define $J(\mathbf{x},\mathbf{y})$ as the d-dimensional rectangle with opposite corners at $\mathbf{x}$ and $\mathbf{y}$. The classical definition (Roth, 1954; Zaremba, 1968; Halton and Zaremba, 1969) of the *root mean square* or L^2 *discrepancy*, is

$$T_N^*(S) = \left\{ \int_{I^d} [R_N(J(0,\mathbf{x}))]^2 \, d\mathbf{x} \right\}^{1/2}.$$

An explicit formula for this discrepancy is (Morokoff and Caflisch, 1994; Tuffin, 1996)

$$[T_N^*(S)]^2 = \frac{1}{N^2} \sum_{n=1}^{N} \sum_{m=1}^{N} \prod_{i=1}^{d} [1 - \max(x_n^i, x_m^i)] - \frac{1}{2^{d-1} N} \sum_{n=1}^{N} \prod_{i=1}^{d} (1 - x_n^{i\,2}) + \frac{1}{3^d}. \quad (2)$$

However, as noted in Morokoff and Caflisch (1994), this definition puts an undue amount of emphasis on points near 0, so a better measure for comparing sequences is

$$T_N(S) = \left\{ \int_{(x,y) \in I^d, x_i < y_i} [R_N(J(\mathbf{x},\mathbf{y}))]^2 d\mathbf{x} \, d\mathbf{y} \right\}^{1/2}.$$

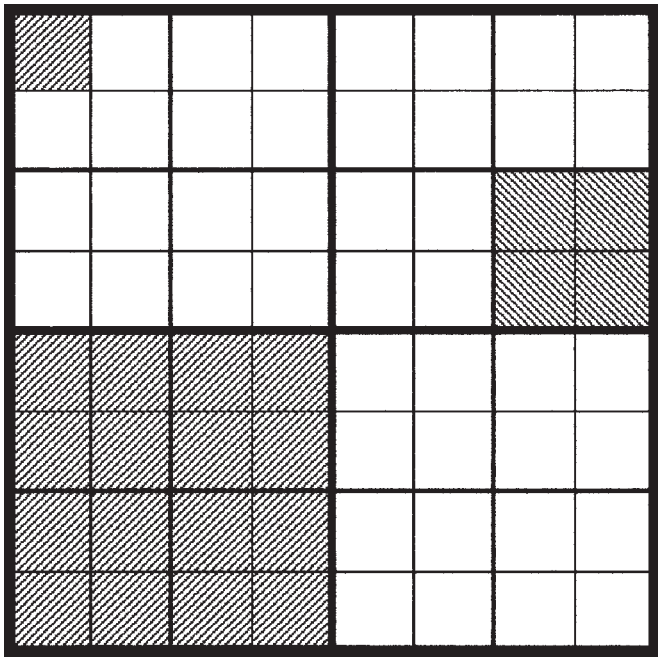

Figure 4. The 64 squares in the Quad-Division of [0, 1] × [0, 1] three times form the class Quad {*R*; 3}.

This integration is over all rectangles in I^d instead of only those with a corner at 0. An explicit formula for this discrepancy is given in Morokoff and Caflisch (1994):

$$[T_N(S)]^2 = \frac{1}{N^2}\sum_{n=1}^{N}\sum_{m=1}^{N}\prod_{i=1}^{d}\left[1-\max(x_n^i, x_m^i)\right]\min(x_n^i, x_m^i) - \frac{1}{2^{d-1}N}\sum_{n=1}^{N}\prod_{i=1}^{d}x_n^i(1-x_n^i) + \frac{1}{12^d}. \quad (3)$$

These two classes are natural choices for the originally intended use of the sampling sequences, namely Monte Carlo integration. An alternative class that is appropriate for discretized square images is a nested class of squares used in binary image representations via quad-trees. We define Quad{*R*; *K*} to be the set of 4^K squares of the form $[i/2^K, (i+1)/2^K] \times [j/2^K, (j+1)/2^K]$, $i,j = 0,\ldots, 2^K - 1$. An illustration of Quad{*R*; 3} is shown in Figure 4. The larger squares with heavier borders can be seen to depict the 16 regions of Quad{*R*; 2}, the 4 regions of Quad{*R*; 1}, and the single region consisting of the whole square, or Quad{*R*; 0}. This leads to the definitions of a related set of quad-discrepancies

$$T_N^Q(S;K) = \left\{\frac{1}{2^{2K}}\sum_{i=0}^{2^K-1}\sum_{j=0}^{2^K-1}\left[R_N\left(J\left(\frac{(i,j)}{2^K}, \frac{(i+1,j+1)}{2^K}\right)\right)\right]^2\right\}^{1/2}, \quad (4)$$

and the overall quad-discrepancy is

$$T_N^Q(S) = \left\{\sum_{k=1}^{\infty}\left[T_N^Q(S;k)\right]^2\right\}^{1/2}. \quad (5)$$

D. Traditional Low Discrepancy Sequences. *Low discrepancy sequences* are those for which $T_N^*(S) = O(N^{-1}\log N)$ for $d = 1$ and $T_N^*(S) = O(N^{-1}(\log N)^{\alpha(d)})$ for $d \geq 2$, where $d/2 \leq \alpha(d) \leq d$ (Niederreiter, 1992; Bouleay and Lépingle, 1994; Tuffin, 1996). Roth (1954) proved that

$$T_N^*(S) > \frac{(\log_2 N)^{(d-1)/2}}{2^{2d+4}\,(d-1)^{(d-1)/2}\,N} \quad (6)$$

for $d \geq 2$, thereby providing a lower bound on the irregularity of the distribution of *S*.

Since we are interested in 2-dimensional images, we will confine our attention to the case $d = 2$. Thus we will let $\mathbf{x} = (x, y)$. In this case, the explicit formula (3) becomes

$$[T_N(S)]^2 = \frac{1}{N^2}\sum_{n=1}^{N}\sum_{m=1}^{N}[1-\max(x_n,x_m)]\min(x_n,x_m) \times[1-\max(y_n,y_m)]\min(y_n,y_m) - \frac{1}{2N}\sum_{n=1}^{N}(1-x_n)x_n(1-y_n)y_n + \frac{1}{144}. \quad (7)$$

The Roth lower bound (6) is in this case given by

$$T_N^*(S) > \frac{(\log_2 N)^{1/2}}{2^8 N}, \quad (8)$$

and (2) can be written as

$$[T_N^*(S)]^2 = \frac{1}{N^2}\sum_{n=1}^{N}\sum_{m=1}^{N}[1-\max(x_n,x_m)][1-\max(y_n,y_m)] - \frac{1}{2N}\sum_{n=1}^{N}(1-x_n^2)(1-y_n^2) + \frac{1}{9}. \quad (9)$$

In Vilenkin (1967) and Halton and Zaremba (1969), explicit low discrepancy sequences were obtained for which

$$T_N^* = \frac{\left[\frac{(\log_2 N)^2}{64} + \frac{29\log_2 N}{192} + \frac{3}{8} - \frac{\log_2 N}{16N} + \frac{1}{4N} - \frac{1}{72N^2}\right]^{1/2}}{N} \quad (10)$$

when *N* is a positive power of 2. These sequences, the so-called Halton sequences, are seen to attain the asymptotic behavior of $(\log_2 N)/(2^8 N)$.

The expected discrepancies for a 2-D random sequence are (Morokoff and Caflisch, 1994)

$$E(T_N^*) = \frac{\sqrt{5}}{6\sqrt{N}}$$

and

$$E(T_N^*) = \frac{\sqrt{3}}{12\sqrt{N}}.$$

Thus it is possible to construct sequences of significantly lower discrepancy than by choosing points at random.

E. Quad Discrepancies. A sequence of *N* points can attain the lowest possible Quad discrepancy if for any positive integer *k* such

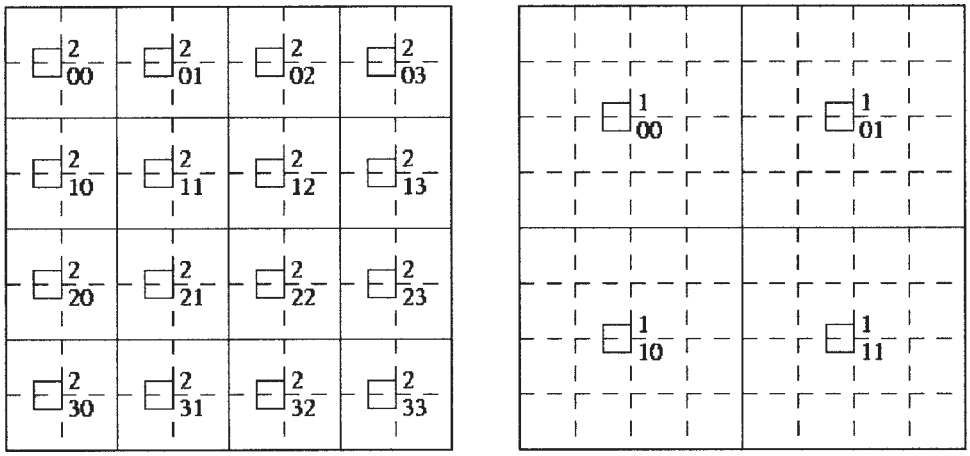

Figure 5. Decomposing the image into disjoint blocks.

that $4^k \le N$, each of the first 4^k points lies in a different square of Quad$\{R; k\}$. Then all the points must also lie in different squares of Quad$\{R; k+1\}$, where k is the greatest integer less than or equal to $\log_4 N$. If this is the case, then the contribution to the Quad discrepancy of a sequence of length 4^K is zero for each of the first K terms of (5). For $k > K$, each of the points is necessarily in a different square of Quad$\{R; k\}$. Thus, the Quad discrepancy can be calculated as

$$\left[T_N^Q(S)\right]^2 = \sum_{k=0}^{\infty}\left[T_N^Q(S;k)\right]^2 = \sum_{k=K+1}^{\infty}\left[T_N^Q(S;k)\right]^2$$
$$= \sum_{k=K+1}^{\infty}\frac{1}{2^{2k}}\left[\left(2^{2k}-2^{2K}\right)\left(-\frac{1}{2^{2k}}\right)^2 + 2^{2K}\left(\frac{1}{2^{2k}}-\frac{1}{2^{2k}}\right)^2\right]$$
$$= \sum_{k=K+1}^{\infty}\left(2^{-2K-2k}-2^{-4k}\right) = \frac{4}{15\cdot 2^{4K}} = \frac{4}{15N^2}$$

Thus for $N = 2^{2K}$ this is

$$T_N^Q(S) = \frac{2}{\sqrt{15}\,N},$$

and we see that the minimal Quad discrepancy is of order $O(1/N)$.

III. HOLOGRAPHIC SELF-SIMILAR SAMPLING PROCESSES

A. Ways to Combat the Clumping Effects. Several authors have developed image sampling sequences designed to avoid clumping effects. In addition to those mentioned above for constructing sequences of low discrepancy, a "farthest point strategy" has been used (Eldar et al., 1997; Lagarias, 2000), where each successive point is placed at a position as far away as possible from all the previously placed points. Here we combat clumping effects by ensuring that any sequence of length 4^K has exactly one point in each of the squares of Quad$\{R; K\}$, for any K.

B. Holographic Self-Similar Sampling. In Bruckstein et al. (1998), we considered the following procedure to order the pixels in a square of size $2^K \times 2^K$. The rows and columns are numbered from 0 to $2^K - 1$. Define $\square_{kl}^{M}$ to be the $2^{K-M} \times 2^{K-M}$ square array of pixels whose upper left corner is at row $2^{K-M}\,k$ and column $2^{K-M}\,l$. Thus $\square_{kl}^{M}$ comprises the pixels with row index in $\{2^{K-M}k,\ldots, 2^{K-M}(k+1)-1\}$ and column index in $\{2^{K-M}l, \ldots, 2^{K-M}(l+1)-1\}$. Examples for $K = 3$ and $M = 2, 1$ are illustrated in Figure 5.

A basic sampling pattern for square images is illustrated in Figure 6. Given four pixels in a 2×2 square, we put them in the order upper left, lower right, upper right, and lower left. This pattern is then iterated for larger squares, producing a recursive, or self-similar, sampling sequence. The complete pixel orderings for squares of sides 2, 4, and 8 are shown in Figure 7.

The goal was to order the pixels in such a way that exactly one element of any sequence of 4^M consecutive integers appears in each of the $\square_{kl}^{M}$. This can be accomplished in many ways. However, if there was too much of a pattern in the ordering, aliasing effects were observed, especially when sampling regular patterns in images. Thus instead of a uniform order, our goal of disorderly but systematic holographic sampling was accomplished by the following "jittering" algorithm that mixes up permutations of [0, 1, 2, 3].

Define the permutation functions on {0, 1, 2, 3} as follows:

$$\begin{array}{llll} h_{6i+1}(0)=0 & h_{6i+1}(1)=1 & h_{6i+1}(2)=2 & h_{6i+1}(3)=3 \\ h_{6i+2}(0)=0 & h_{6i+2}(1)=2 & h_{6i+2}(2)=1 & h_{6i+2}(3)=3 \\ h_{6i+3}(0)=0 & h_{6i+3}(1)=2 & h_{6i+3}(2)=3 & h_{6i+3}(3)=1 \\ h_{6i+4}(0)=0 & h_{6i+4}(1)=1 & h_{6i+4}(2)=3 & h_{6i+4}(3)=2 \\ h_{6i+5}(0)=0 & h_{6i+5}(1)=3 & h_{6i+5}(2)=1 & h_{6i+5}(3)=2 \\ h_{6i+6}(0)=0 & h_{6i+6}(1)=3 & h_{6i+6}(2)=2 & h_{6i+6}(3)=1 \end{array} \tag{11}$$

and $h_i(4k+m) = h_i(m)$ for all nonnegative integers i, k, and m. Also let

$$\begin{array}{lll} g_{6i+1}(n)=h_5(n) & g_{6i+2}(n)=h_3(n) & g_{6i+3}(n)=h_1(n) \\ g_{6i+4}(n)=h_6(n) & g_{6i+5}(n)=h_2(n) & g_{6i+6}(n)=h_4(n) \end{array} \tag{12}$$

for all nonnegative integers i. Next, let

$$f(n,a) = \left[g_{a+1}(n) + \sum_{b=1}^{a} h_{a-b+1}\left(\left\lfloor \frac{n}{4^b}\right\rfloor\right)\right] \pmod 4, \tag{13}$$

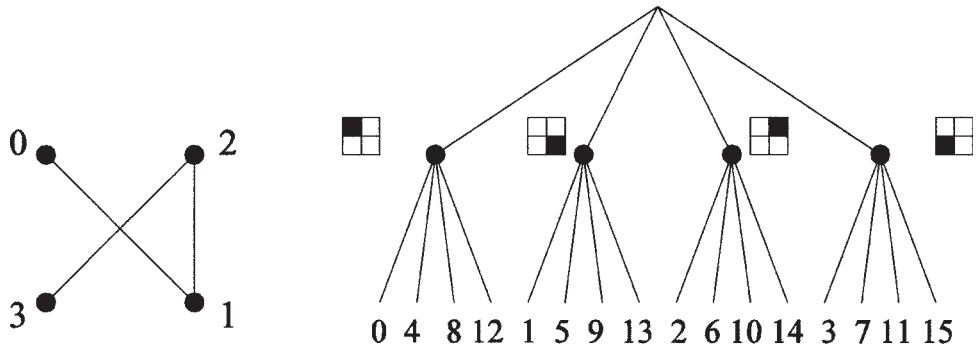

Figure 6. Basic ordering scheme (left) and quad-tree Structure (right).

where $\lfloor \cdot \rfloor$ is the floor function ($\lfloor x \rfloor$ is the greatest integer less than or equal to x), and define

$$r(n,a)=\begin{Bmatrix} 0 \text{ if} f(n,a) \in \{0,1\} \\ 1 \text{ if} f(n,a) \in \{2,3\} \end{Bmatrix} \quad c(n,a)=\begin{Bmatrix} 0 \text{ if} f(n,a) \in \{0,2\} \\ 1 \text{ if} f(n,a) \in \{1,3\} \end{Bmatrix}. \tag{14}$$

Then the integer n is located at pixel (i, j), where

$$i=\sum_{a=0}^{K-1} 2^{K-a-1} r(n,a) \qquad j=\sum_{a=0}^{K-1} 2^{K-a-1} c(n,a). \tag{15}$$

This ordering may be more easily understood with an example. Consider the integer 45 in the third array of Figure 8. The formulas above, with $K = 3$, give

$$\begin{aligned} f(45,0) &= g_1(45) = h_5(1) = 3, \\ f(45,1) &= g_2(45) + h_1(11) = h_3(1) + h_1(3) = 2 + 3 (\text{mod } 4) = 1, \\ f(45,2) &= g_3(45) + h_2(11) + h_1(2) = h_1(1) + h_2(3) + h_1(2) \\ &= 1 + 3 + 2 (\text{mod } 4) = 2. \end{aligned}$$

Thus by (15) the row index for 45 is $2^2 1 + 2^1 0 + 2^0 1 = 5$ and the column index is $2^2 1 + 2^1 1 + 2^0 0 = 6$.

The sequences obtained with this ordering for $K = 1, 2, 3$ are shown in Figure 8.

We now return to the regular holographic sampling that was first described in this section. Using the same notation as (11), we find that equations (14) and (15) hold in this case when in place of (13),

0	2
3	1

0	8	2	10
12	4	14	6
3	11	1	9
15	7	13	5

0	32	8	40	2	34	10	42
48	16	56	24	50	18	58	26
12	44	4	36	14	46	6	38
60	28	52	20	62	30	54	22
3	35	11	43	1	33	9	41
51	19	59	27	49	17	57	25
15	47	7	39	13	45	5	37
63	31	55	23	61	29	53	21

Figure 7. Pixel orderings with uniform sampling for 2 × 2, 4 × 4, and 8 × 8 images.

0	2
3	1

0	4	6	10
8	12	14	2
15	3	9	13
7	11	1	5

0	16	36	52	6	22	26	42
32	48	4	20	38	54	58	10
56	8	28	44	62	14	34	50
24	40	60	12	30	46	2	18
47	63	19	35	41	57	13	29
15	31	51	3	9	25	45	61
55	7	11	27	49	1	21	37
23	39	43	59	17	33	53	5

Figure 8. Pixel orderings with "jittered" sampling for 2 × 2, 4 × 4, and 8 × 8 images.

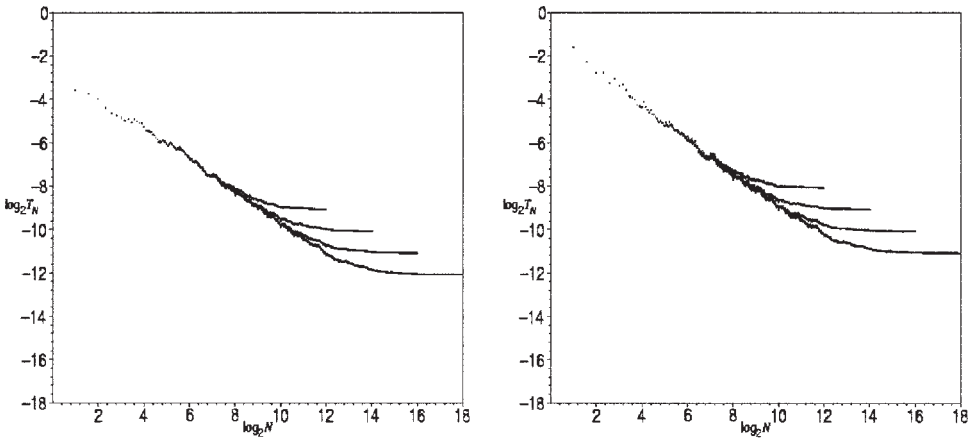

Figure 9. From top to bottom, the graphs are for 64 × 64, 128 × 128, 256 × 256, and 512 × 512 images of the (a) T_N and (b) $T_N^\star$ discrepancies of the jittered sampling sequence with points selected from the center of each pixel given by (13).

$f(n,a)$ is simply defined as

$$f(n,a) = h_5\left(\left\lfloor \frac{n}{4^a} \right\rfloor\right). \tag{16}$$

As an example, consider the integer 27 in the third array of Figure 7. Formulas (11), (16), (14), and (15) yield

$$f(27,0) = h_5(27) = h_5(3) = 2,$$
$$f(27,1) = h_5(6) = h_5(2) = 1,$$
$$f(27,2) = h_5(1) = 3.$$

Thus by (15), the row index for 27 is $2^2 1 + 2^1 0 + 2^0 1 = 5$ and the column index is $2^2 0 + 2^1 1 + 2^0 1 = 3$.

C. The Sample Uniformity Theorem. With either of these orderings we have the following uniformity theorem, whose proof is given in Appendix A.

1. Theorem 1. Let a $2^K \times 2^K$ *array for any* $K \geq 0$ *be numbered according to the rules expressed by* (11), *either* (13) *or* (16), (14), *and* (15). *For M such that* $0 \leq M \leq K$, *divide the array into the* 4^M *disjoint* $2^{K-M} \times 2^{K-M}$ *squares* $\square_{kl}^M$, $k, l \in \{0,\ldots, 2^M - 1\}$. *Then exactly one element of any sequence of* 4^M *consecutive integers in* $[0, 4^K - 1]$ *appears in each of the squares* $\square_{kl}^M$. *The sequence may wrap around, with* 0 *following* $4^K - 1$.

In terms of the Quad discrepancy, the statement of Theorem 1 *is equivalent to*

$$T_N^Q(S;k) = 0, \quad k = 1,\ldots,K.$$

IV. DISCREPANCIES OF VARIOUS SEQUENCES

A. Discrepancies of Subsequences of Self-Similar Holographic Samples.

To relate the pixel orderings of the previous section to point sequences, we will assume that each pixel corresponds to the point in its center. To conform with the established literature, the image will be scaled to a 1 × 1 square. Thus, the coordinates of the nth point are

$$(x_n, y_n) = \left(\frac{i+1/2}{2^K}, \frac{j+1/2}{2^K}\right) = \left(\frac{2i+1}{2^{K+1}}, \frac{2j+1}{2^{K+1}}\right), \tag{17}$$

where $N = 2^{2K}$, and i and j are defined by (11), and (13)–(15) for the jittered sequence and by (11), (16), (14), and (15) for the uniform sequence.

Figure 9 shows the graphs for the T_N and T_N^* discrepancies of the sampling sequence given by (13) for images of varying size. All these graphs show that the errors for the T_N^* discrepancy are greater than those for the corresponding T_N discrepancy. Figure 10

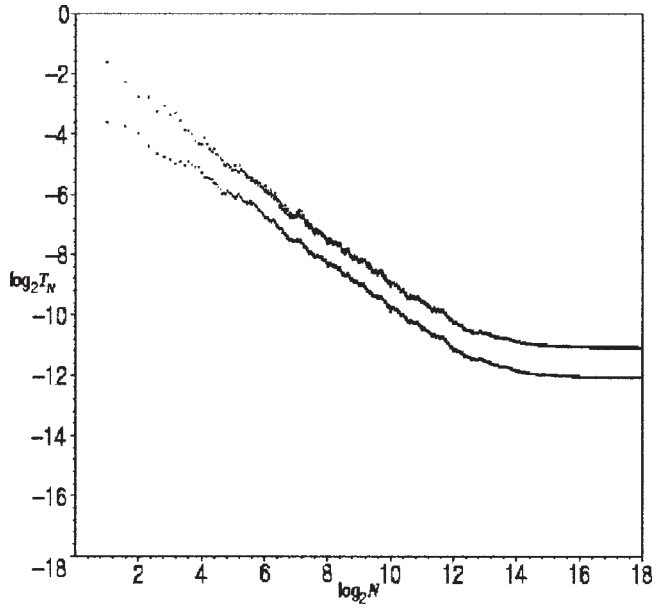

Figure 10. The upper and lower graphs are for the $T_N^\star$ and T_N discrepancies, respectively, of the jittered sampling sequence (13), for the 512 × 512 image.

compares the graphs for the 512×512 images for both the T_N and T_N^* discrepancies. As is the case in Morokoff and Caflisch (1994), the graphs of the T_N and T_N^* discrepancies usually are nearly parallel for $N > 50$ or so, with that for the T_N being smaller. In fact, the difference between the two graphs approaches 1 unit in the $\log_2 - \log_2$ plot at the endpoint, as will now be shown.

Because of symmetry in the placement of the points, the double summation in (7) equals

$$\left\{\sum_{n=1}^{N}\sum_{m=1}^{N}[1-\max(x_n,x_m)]\ \min(x_n,x_m)\right\}^2.$$

(Note: in the literature, sequences sometimes start at $\mathbf{x}_0$ and sometimes at $\mathbf{x}_1$. To allow for this, the point $\mathbf{x}_N$ in the latter is identified with $\mathbf{x}_0$ in the former.)

The x_n and y_n are all of the form $(2i+1)/2^{K+1}$ for $0 \le i < 2^K$, where $N = 2^{2K}$. Next, this double sum is equivalent to

$$2\sum_{i=0}^{2^K-2}\sum_{j=0}^{2^K-i-2}\left(\frac{2i+1}{2^{K+1}}\right)\left(\frac{2j+1}{2^{K+1}}\right)+\sum_{i=0}^{2^K-1}\left(\frac{2i+1}{2^{K+1}}\right)\left(\frac{2^{K+1}-2i-1}{2^{K+1}}\right)=\frac{2^{2K}}{12}+\frac{1}{6}.$$

The single summation in (7) is equivalent to

$$\left[\sum_{i=0}^{2^K-1}\left(\frac{2i+1}{2^{K+1}}\right)\left(\frac{2^{K+1}-2i-1}{2^{K+1}}\right)\right]^2=\left(\frac{2^K}{6}+\frac{2^{-K}}{12}\right)^2.$$

Combining these shows that the value of (7) for a complete $2^K \times 2^K$ grid is

$$\frac{1}{2^{4K}}\left(\frac{2^{2K}}{12}+\frac{1}{6}\right)^2-\frac{1}{2^{2K+1}}\left(\frac{2^K}{6}+\frac{2^{-K}}{12}\right)^2+\frac{1}{144}=\frac{2^{-2K}}{72}+\frac{7\cdot 2^{-4K}}{288}=\frac{4N+7}{288N^2}.$$

Consequently, we have

$$T_N(S)=\frac{\sqrt{4N+7}}{12\sqrt{2}\sqrt{N}}\approx\frac{1}{6\sqrt{2}\sqrt{N}}\qquad\text{for large } N. \tag{18}$$

Again due to symmetry in the placement of the points, the double summation in (9) equals

$$\left\{\sum_{n=1}^{N}\sum_{m=1}^{N}[1-\max(x_n,x_m)]\right\}^2.$$

Next, this double sum is equivalent to

$$2\sum_{i=0}^{2^K-2}\sum_{j=0}^{2^K-i-2}\left(\frac{2i+1}{2^{K+1}}\right)+\sum_{i=0}^{2^K-1}\left(\frac{2i+1}{2^{K+1}}\right)=\frac{2^{2K}}{3}+\frac{1}{6}.$$

The single summation in (9) is equivalent to

$$\left[\sum_{i=0}^{2^K-1}\left(\frac{2i+1}{2^{K+1}}\right)\right]^2=\left(\frac{2\cdot 2^K}{3}+\frac{2^{-K}}{12}\right)^2.$$

Combining these shows that the value of (9) for a complete $2^K \times 2^K$ grid is

$$\frac{1}{2^{4K}}\left(\frac{2^{2K}}{3}+\frac{1}{6}\right)^2-\frac{1}{2^{2K+1}}\left(\frac{2\cdot 2^K}{3}+\frac{2^{-K}}{12}\right)^2+\frac{1}{144}=\frac{2^{-2K}}{18}+\frac{7\cdot 2^{-4K}}{288}=\frac{16N+7}{288N^2}.$$

Consequently, we have

$$T_N^*(S)=\frac{\sqrt{16N+7}}{12\sqrt{2}\sqrt{N}}\approx\frac{1}{3\sqrt{2}\sqrt{N}}\qquad\text{for large } N. \tag{19}$$

Thus for a filled $2^K \times 2^K$ grid, the value of the T_N and T_N^* discrepancies for $N = 4^K$ are extremely close to $(6\sqrt{2}\ 2^K)^{-1} \approx 2^{-K+3.085}$ and $(3\sqrt{2}\ 2^K)^{-1} \approx 2^{-K+2.085}$ respectively. These approximations are borne out in Figure 10.

Equations (18) and (19) provide upper bounds on the discrepancies of sequences that satisfy the hypotheses of Theorem 1. These bounds are $\sqrt{2/3} = 0.816$ and $\sqrt{2/5} = 0.632$ for the corresponding expected discrepancies of random sequences. However, as seen from the graphs, especially Figure 12b, the holographic sequence described by (13) fares much better in low discrepancy terms when the number of points taken is up to 1/64 of the total number of pixels.

By construction, the holographic sequences described in the previous section (by (11), either (13) or (16), (14), and (15)) satisfy the hypotheses of Theorem 1 and have the property that any subsequence of length 4^K has exactly one point in each of the squares of Quad$\{R; K\}$, or $\square_{kl}^0$. Therefore, these sequences achieve the minimum possible Quad discrepancy discussed in Section II.E.

The Halton sequence and several of its modifications (Halton and Zaremba, 1969; Warnock, 1972; Braaten and Weller, 1979; Niederreiter, 1992; Morokoff and Caflisch, 1994; Tuffin, 1996; Kocis and Whiten, 1997; Wong et al., 1997) also attain this minimal Quad Discrepancy if the appropriate two edges are considered to be part of the squares of Quad$\{R; K\}$. The original Halton sequence may be defined as follows (Wong et al., 1997). If the positive integer k has the binary representation $k = a_0 + 2a_1 + 2^2 a_2 + \cdots + 2^r a_r$, then $\phi_2(k) = a_0 / 2 + a_1 / 2^2 + \cdots + a_r / 2^{r+1}$. The Halton sequence of length n is then $\{(k / n, \phi_2(k))\}$. The sequence of length 16 is shown in Figure 11.

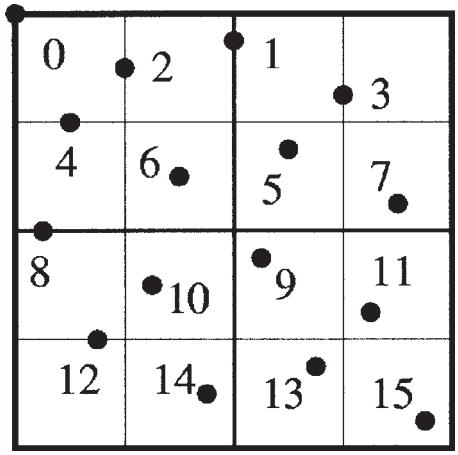

Figure 11. Halton sequence of length 16. This has minimal quad-discrepancy if each cell is considered to contain its top and left edges.

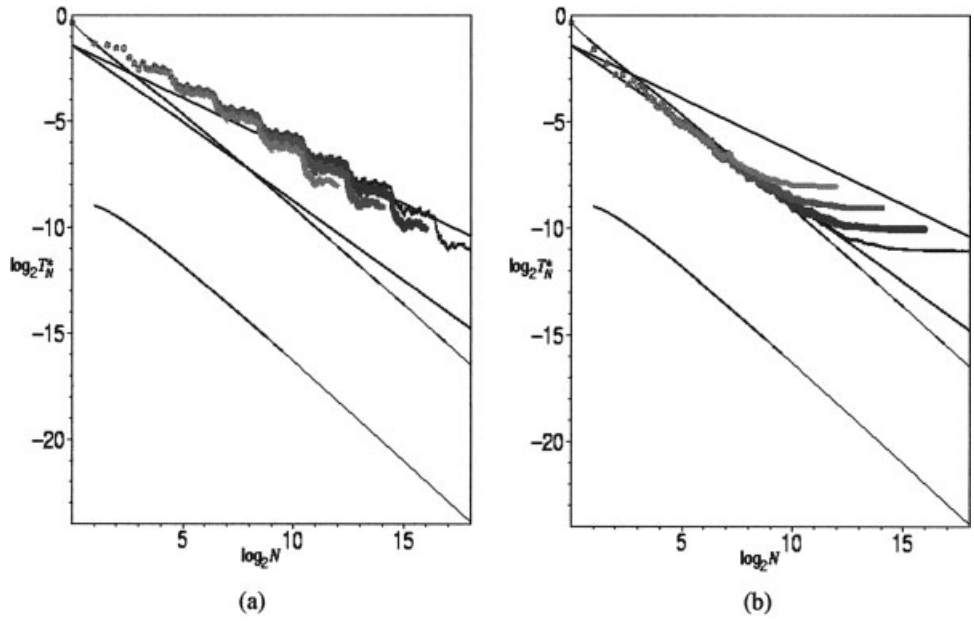

Figure 12. T_N^* discrepancies of the (a) uniform and (b) jittered sampling sequences for 64 × 64, 128 × 128, 256 × 256, and 512 × 512 images, with points selected from the center of each pixel given by (16) and (13), respectively. The nearly straight lines represent, from top to bottom at the right edges, the expected discrepancy for a totally random sequence, the expected discrepancy for a sequence with points placed at random within each pixel, the Halton sequence, and the lower bound of Roth.

Modified Halton sequences involve scrambling the order of the rows, and using different prime bases in the representation of positive integers. However, these sequences do not have the holographic property, i.e., that *every* subsequence of length 4^K contains one point in each of the Quad{R; K}, or $\square_{kl}^0$. Their construction is ideal for their intended purpose of simulated Monte Carlo integration, but does not meet the uniformity standards we seek for holographic image sampling.

Since the T_N^* discrepancy has received much more attention in the literature and is more available for comparisons, we will show mainly comparisons of T_N^* discrepancies rather than T_N in the rest of this paper.

B. Regular Grid with Random Placement Within Cells. In this section, we compute the expected value of the discrepancy (9) for a complete $2^K \times 2^K$ grid when the points are chosen randomly and uniformly from each pixel. We number the cells from top to bottom and then from left to right. Thus if $n = 2^K i + j$, where $0 \le i, j \le 2^K - 1$, the nth cell, in which we place the nth point, is in the in the ith column and jth row. The coordinates of the nth point are then

$$(x_n, y_n) = \left(x_{2^K i+j}, y_{2^K i+j}\right) = \left(\frac{i}{2^K} + \frac{1}{2^{K+1}} + \varepsilon_{2^K i+j}, \frac{j}{2^K} + \frac{1}{2^{K+1}} + \delta_{2^K i+j}\right),$$

where the ε_n and δ_n are random variables uniformly distributed on $[-1/2^{K+1}, 1/2^{K+1}]$. We define $f_1(i_1,i_2,j_1,j_2)$ and $f_2(i_1,i_2,j_1,j_2)$ to be the expected value of the first and second summations of (9) (leaving out the factors of $1/N^2$ and $-1/(2N)$). After a lengthy calculation given in Appendix B, we find that the expected squared error of the T_N^* discrepancy is

$$\frac{1}{N^2} f_1(i_1,i_2,j_1,j_2) - \frac{1}{2N} f_2(i_1,i_2,j_1,j_2) + \frac{1}{9} = \frac{1}{6\cdot 2^{3K}} - \frac{1}{36\cdot 2^{4K}},$$

or

$$E(T_N^*) = \sqrt{\frac{1}{6N^{3/2}} - \frac{1}{36N^2}}, \tag{20}$$

valid for N being an even power of 2. Thus for large N, the expected discrepancy is asymptotic to $1/\sqrt{6}\, N^{3/4}$. This is illustrated in Figures 12 and 13, where the slope of the graph of this discrepancy on the log–log plots is close to $-3/4$. This curve crosses that for the Halton sequence (10) near $N = 2^8$.

For comparison purposes, upon a slightly more complicated calculation given in Appendix C, the expected squared error of the T_N discrepancy is found to be

$$\frac{1}{N^2} g_1(i_1,i_2,j_1,j_2) - \frac{1}{2N} g_2(i_1,i_2,j_1,j_2) + \frac{1}{144} = \frac{1}{18\cdot 2^{3K}} - \frac{1}{18\cdot 2^{4K}} + \frac{1}{36\cdot 2^{5K}} - \frac{1}{144\cdot 2^{6K}},$$

or

$$E(T_N) = \sqrt{\frac{1}{18N^{3/2}} - \frac{1}{18N^2} + \frac{1}{36N^{5/2}} - \frac{1}{144N^3}}, \tag{21}$$

where $g_1(i_1,i_2,j_1,j_2)$ and $g_2(i_1,i_2,j_1,j_2)$ are the expected value of the first and second summations of (7) (leaving out the factors of $1/N^2$ and $-1/(2N)$). Asymptotically, the T_N discrepancy is lower by a factor of $\sqrt{3}$ than the T_N^* discrepancy.

In the following four Figures 12a, and 12b, 13a and 13b, graphs of various T_N^* discrepancies are shown, along with four fixed curves. From largest to smallest at $\log_2 N \ge 12$, these are the expected discrepancy for a totally random sequence, the expected discrepancy for a sequence with points placed at random within

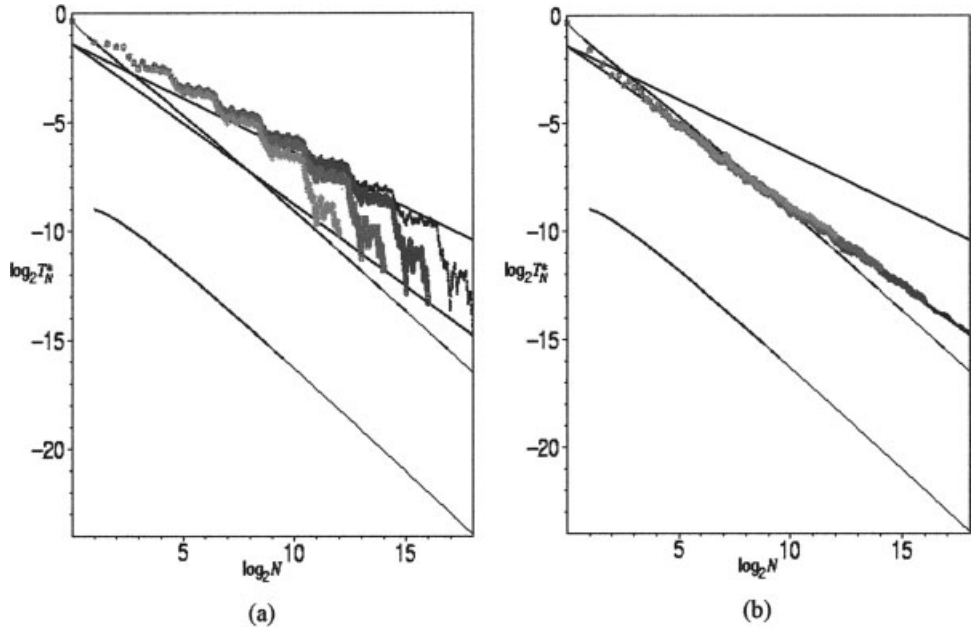

Figure 13. T_N^* discrepancies of the (a) uniform and (b) jittered sampling sequences for 64 × 64, 128 × 128, 256 × 256, and 512 × 512 images, with points selected at random from within each pixel given by (16) and (13), respectively. The nearly straight lines represent, from top to bottom at the right edges, the expected discrepancy for a totally random sequence, the expected discrepancy for a sequence with points placed at random within each pixel, the Halton sequence, and the lower bound of Roth.

each pixel, the Halton sequence (10), and the lower bound of Roth (8). The first two of these are valid for integer values of $\log_2 N \geq 12$, and the third for even integer values of $\log_2 N \geq 12$, but smooth curves are drawn through the points with integer arguments. The graphs for 64 × 64, 128 × 128, 256 × 256, and 512 × 512 may be distinguished by the increasing darkness of the plots, and the fact they the end at $\log_2 N = 12$, 14, 16, and 18, respectively.

Figure 12 shows the graphs of the T_N^* discrepancy of the uniform and jittered sampling sequences given by (16) and (13), respectively, for 64 × 64, 128 × 128, 256 × 256, and 512 × 512 arrays. The points are placed at the centers of the appropriate pixels. The graphs in Figure 12b are quite close to those of the 2-dimensional Hammersley-Halton sequence (Morokoff and Caflisch, 1994) for N up to 2^8, 2^9, 2^{10}, and 2^{11}, respectively, and then they level off instead of continuing downward in an $O(1/N)$ manner. Figures 12a and 12b also show the large benefit induced by the jittering of the pixels selected for the sampling sequence.

Figure 13 shows the graphs of the T_N^* discrepancy of the uniform and jittered sampling sequences for 64 × 64, 128 × 128, 256 × 256, and 512 × 512 arrays, with the points being randomly selected from within pixels given by (16) and (13), respectively. Again, Figures 13a and 13b show the large benefit induced by the "jittering" of the pixels selected for the sampling sequence. With the jittering the discrepancy of the sequence in Figure 12b is very close to the expected value given by (20) for all values of N, not just integer powers of 2.

Figure 14 shows graphs for 512 × 512 images for the T_N discrepancy. The top graph is for the point sequence discussed above, and the bottom graph is for the sequence where the point is chosen at random from the appropriate pixel instead at its center.

V. CONCLUSIONS

As we have seen in the experiments, the pixel orderings used in Bruckstein et al. (1998) for the holographic representation of images may be regarded as low discrepancy sequences. Since these orderings have a recursive definition, they may be described as self-similar. The discrepancies for a $2^K \times 2^K$ image using the center of each pixel are quite similar to those for Halton sequences through approximately 2^{K+2} points before leveling off. The leveling off phenomenon vanishes, and the discrepancy decreases as $1 / N^{3/4}$, if one can pick points at random from within each pixel for the points

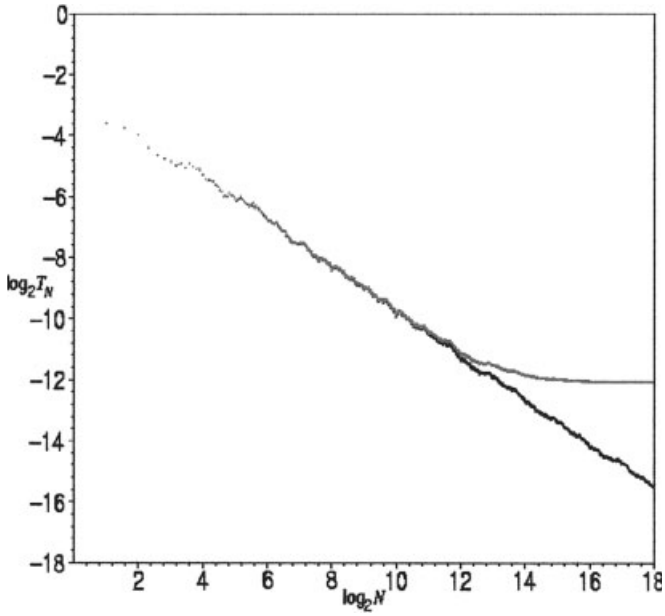

Figure 14. T_N discrepancies for the 512 × 512 image. The upper and lower graphs are for the original jittered sequence, with points selected at the center of each pixel, and a sequence where points are chosen at random from within each pixel.

of the sampling sequence. We believe that the good properties of the holographic sampling sequences discussed above both in terms of discrepancy and in terms of their resilience to loss of arbitrary portions of the sampled data make them the most natural candidates for streaming images over sequential channels.

APPENDIX

A. Proof of Uniformity Theorem. Here we prove Theorem 1 of Section III for the more difficult case of the "jittered" sampling. The proof for the uniform sampling is very similar.

1. Proof. This result will be proved by showing that all the integers contained in any square $\square_{kl}^{M}$ are congruent modulo 4^M. Equivalently, any two integers congruent to each other modulo 4^M must lie in the same square $\square_{kl}^{M}$. Suppose $n_1 \equiv n_2 \pmod{4^M}$. Then $n_1/4^{M-1} \equiv n_2/4^{M-1} \pmod 4$, and by (13), $f(n_1, a) = f(n_2, a)$ for $a = 0,\ldots, M-1$. Then by (14), $r(n_1, a) = r(n_2, a)$ and $c(n_1, a) = c(n_2, a)$ for $a = 0,\ldots, M-1$, and by (15), the first $M-1$ binary digits of i_1 and i_2 are identical, as are those for j_1 and j_2, where (i_1, j_1) and (i_2, j_2) are the pixels at which n_1 and n_2 are located. This implies that (i_1, j_1) and (i_2, j_2) are both located in $\square_{kl}^{M}$, where $k = \Sigma_{a=0}^{M-1} 2^{M-1-a}\, r(n, a)$, $l = \Sigma_{a=0}^{M-1} 2^{M-1-a}\, c(n, a)$, and n is either n_1 or n_2.

Thus each k and l, $\square_{kl}^{M}$ contains 4^{K-M} integers in $[0, 4^N - 1]$ that are congruent to each other. Since there are 4^M such squares, there is a one-to-one correspondence between these squares and the sets of 4^{K-M} integers in $[0,4^N - 1]$, which are congruent to each other modulo 4^M. Therefore, every integer sequence of length 4^M (including wrap-around sequences) has exactly one element in each $\square_{kl}^{M}$. ■

B. Proof of Equation (20). Here we prove (20),

$$E(T_N^*) = \sqrt{\frac{1}{6N^{3/2}} - \frac{1}{36N^2}},$$

for the sequence given by (13) with points selected at random from within each pixel.

We start with the definitions

$$f_1(i_1,i_2,j_1,j_2) = E\left(\sum_{n=1}^{N}\sum_{m=1}^{N}[1-\max(x_n,x_m)][1-\max(y_n,y_m)]\right)$$

$$f_2(i_1,i_2,j_1,j_2) = E\left(\sum_{n=1}^{N}(1-x_n^2)(1-y_n^2)\right)$$

$$x_n = \frac{i}{2^K} + \frac{1}{2^{K+1}} + \varepsilon_{2^K i+j}$$

$$y_n = \frac{j}{2^K} + \frac{1}{2^{K+1}} + \delta_{2^K i+j} \quad \text{where } n = 2^K i + j.$$

Then we use the results

$$\int_{-\frac{1}{2^{K+1}}}^{\frac{1}{2^{K+1}}}\left(\frac{i}{2^K} + \frac{1}{2^{K+1}} + \varepsilon\right)d\varepsilon = \frac{2i+1}{2^{2K+1}}$$

and

$$\int_{-\frac{1}{2^{K+1}}}^{\frac{1}{2^{K+1}}}\int_{-\frac{1}{2^{K+1}}}^{\frac{1}{2^{K+1}}}\left[\frac{i}{2^K} + \frac{1}{2^{K+1}} + \max(\varepsilon_1,\varepsilon_2)\right]d\varepsilon_2\, d\varepsilon_1$$

$$= \int_{-\frac{1}{2^{K+1}}}^{\frac{1}{2^{K+1}}}\int_{-\frac{1}{2^{K+1}}}^{\varepsilon_1}\left(\frac{i}{2^K} + \frac{1}{2^{K+1}} + \varepsilon_1\right)d\varepsilon_2\, d\varepsilon_1$$

$$+ \int_{-\frac{1}{2^{K+1}}}^{\frac{1}{2^{K+1}}}\int_{\varepsilon_1}^{\frac{1}{2^{K+1}}}\left(\frac{i}{2^K} + \frac{1}{2^{K+1}} + \varepsilon_2\right)d\varepsilon_2\, d\varepsilon_1 = \frac{3i+2}{3\cdot 2^{3K}}.$$

This gives us

$$f_1(i_1,i_2,j_1,j_2) = 2^{K4^K}\int_{-\frac{1}{2^{K+1}}}^{\frac{1}{2^{K+1}}}\cdots\int_{-\frac{1}{2^{K+1}}}^{\frac{1}{2^{K+1}}}[1-\max(x_{2^K i_1+j_1}, x_{2^K i_2+j_2})]$$
$$\times[1-\max(y_{2^K i_1+j_1}, y_{2^K i_2+j_2})]\, d\varepsilon_0 \ldots d\varepsilon_{2^K-1}\, d\delta_0 \ldots d\delta_{2^K-1}$$

$$= \begin{cases} \left(1-\frac{2i_1+1}{2^{K+1}}\right)\left(1-\frac{2j_1+1}{2^{K+1}}\right) & i_1 > i_2,\ j_1 > j_2 \\ \left(1-\frac{2i_1+1}{2^{K+1}}\right)\left(1-\frac{2j_2+1}{2^{K+1}}\right) & i_1 > i_2,\ j_1 < j_2 \\ \left(1-\frac{2i_1+1}{2^{K+1}}\right)\left(1-\frac{3j_1+2}{3\cdot 2^K}\right) & i_1 > i_2,\ j_1 = j_2 \\ \left(1-\frac{2i_2+1}{2^{K+1}}\right)\left(1-\frac{2j_1+1}{2^{K+1}}\right) & i_1 < i_2,\ j_1 > j_2 \\ \left(1-\frac{2i_2+1}{2^{K+1}}\right)\left(1-\frac{2j_2+1}{2^{K+1}}\right) & i_1 < i_2,\ j_1 < j_2 \\ \left(1-\frac{2i_2+1}{2^{K+1}}\right)\left(1-\frac{3j_1+2}{3\cdot 2^K}\right) & i_1 < i_2,\ j_1 = j_2 \\ \left(1-\frac{3i_1+1}{3\cdot 2^K}\right)\left(1-\frac{2j_1+1}{2^{K+1}}\right) & i_1 = i_2,\ j_1 > j_2 \\ \left(1-\frac{3i_1+1}{3\cdot 2^K}\right)\left(1-\frac{2j_2+1}{2^{K+1}}\right) & i_1 = i_2,\ j_1 < j_2 \\ \left(1-\frac{2i_1+1}{2^{K+1}}\right)\left(1-\frac{2j_1+1}{2^{K+1}}\right) & i_1 = i_2,\ j_1 = j_2 \end{cases}.$$

Making use of some symmetry, the sum of these $f_1(i_1,i_2,j_1,j_2)$ is found to be

$$\sum_{i_1=0}^{2^K-1}\sum_{i_2=0}^{2^K-1}\sum_{j_1=0}^{2^K-1}\sum_{j_2=0}^{2^K-1} f_1(i_1,i_2,j_1,j_2)$$

$$= 4\sum_{i_1=0}^{2^K-1}\sum_{i_2=0}^{i_1-1}\sum_{j_1=0}^{2^K-1}\sum_{j_2=0}^{j_1-1}\left(1-\frac{2i_1+1}{2^{K+1}}\right)\left(1-\frac{2j_1+1}{2^{K+1}}\right)$$

$$+ 4\sum_{i_1=0}^{2^K-1}\sum_{i_2=0}^{i_1-1}\sum_{j_1=0}^{2^K-1}\left(1-\frac{2i_1+1}{2^{K+1}}\right)\left(1-\frac{3j_1+2}{3\cdot 2^K}\right)$$

$$+ \sum_{i_1=0}^{2^K-1}\sum_{j_1=0}^{2^K-1}\left(1-\frac{2i_1+1}{2^{K+1}}\right)\left(1-\frac{2j_1+1}{2^{K+1}}\right)$$

$$= 4\left(\frac{2^{4K}}{36} - \frac{2^{3K}}{12} + \frac{13\cdot 2^{2K}}{144} - \frac{2^K}{24} + \frac{1}{144}\right)$$

$$+ 4\left(\frac{2^{3K}}{12} - \frac{11\cdot 2^{2K}}{72} + \frac{2^K}{12} - \frac{1}{72}\right) + \frac{2^{2K}}{4}$$

$$= \frac{2^{4K}}{9} + \frac{2^K}{6} - \frac{1}{36}$$

For the second summation, we use the result

$$\int_{-\frac{1}{2^{K+1}}}^{\frac{1}{2^{K+1}}}\left[1-\left(\frac{i}{2^K} + \frac{1}{2^{K+1}} + \varepsilon\right)^2\right]d\varepsilon = \frac{1}{2^K} - \frac{3i^2+3i+1}{3\cdot 2^{3K}}$$

to get

$$f_2(i_1,i_2,j_1,j_2) = 2^{K4^K}\int_{-\frac{1}{2^{K+1}}}^{\frac{1}{2^{K+1}}}\cdots\int_{-\frac{1}{2^{K+1}}}^{\frac{1}{2^{K+1}}}(1-x_{2^K i_1+j_1}^2)$$
$$\times(1-y_{2^K i_1+j_1}^2)\; d\varepsilon_0\ldots d\varepsilon_{2^K-1}\, d\delta_0\ldots d\delta_{2^K-1}$$
$$=\left(1-\frac{3i^2+3i+1}{3\cdot 2^{2K}}\right)\left(1-\frac{3j^2+3j+1}{3\cdot 2^{2K}}\right).$$

The sum of the $f_2(i_1,i_2,j_1,j_2)$ is then

$$\sum_{i=0}^{2^K-1}\sum_{j=0}^{2^K-1} f_2(i_1,i_2,j_1,j_2) = \sum_{i=0}^{2^K-1}\sum_{j=0}^{2^K-1}\left(1-\frac{3i^2+3i+1}{3\cdot 2^{2K}}\right)\left(1-\frac{3j^2+3j+1}{3\cdot 2^{2K}}\right)$$
$$=\frac{4\cdot 2^{2K}}{9}.$$

Putting these together shows that the expected squared error of the T_N^* discrepancy for this sequence of points is

$$\frac{1}{2^{4K}}\left(\frac{2^{4K}}{9}+\frac{2^K}{6}-\frac{1}{36}\right)-\frac{1}{2\cdot 2^{2K}}\left(\frac{4\cdot 2^{2K}}{9}\right)+\frac{1}{9}=\frac{1}{6\cdot 2^{3K}}-\frac{1}{36\cdot 2^{4K}},$$

so

$$E(T_N^*)=\sqrt{\frac{1}{6N^{3/2}}-\frac{1}{36N^2}},$$

valid for N being an even power of 2. ■

C. Proof of Equation (21). Here we prove (21),

$$E(T_N)=\sqrt{\frac{1}{18N^{3/2}}-\frac{1}{18N^2}+\frac{1}{36N^{5/2}}-\frac{1}{144N^3}},$$

for the sequence given by (13) with points selected at random from within each pixel. We start with the definitions

$$g_1(i_1,i_2,j_1,j_2) = E\left(\sum_{n=1}^{N}\sum_{m=1}^{N}[1-\max(x_n,x_m)]\;\min(x_n,x_m)\right.$$
$$\left.\times[1-\max(y_n,y_m)]\;\min(y_n,y_m)\right)$$
$$g_2(i_1,i_2,j_1,j_2) = E\left(\sum_{n=1}^{N}(1-x_n)x_n(1-y_n)y_n\right)$$
$$x_n=\frac{i}{2^K}+\frac{1}{2^{K+1}}+\varepsilon_{2^K i+j}$$
$$y_n=\frac{j}{2^K}+\frac{1}{2^{K+1}}+\delta_{2^K i+j}\quad\text{where } n=2^K i+j \text{ as before.}$$

Then we use the results

$$\int_{-\frac{1}{2^{K+1}}}^{\frac{1}{2^{K+1}}}\left[1-\left(\frac{i}{2^K}+\frac{1}{2^{K+1}}+\varepsilon\right)\right]\left(\frac{i}{2^K}+\frac{1}{2^{K+1}}+\varepsilon\right)\,d\varepsilon$$
$$=\frac{2i+1}{2\cdot 2^{2K}}-\frac{3i^2+3i+1}{3\cdot 2^{3K}},$$

$$\int_{-\frac{1}{2^{K+1}}}^{\frac{1}{2^{K+1}}}\int_{-\frac{1}{2^{K+1}}}^{\frac{1}{2^{K+1}}}\left[1-\left(\frac{i_1}{2^K}+\frac{1}{2^{K+1}}+\varepsilon_1\right)\right]\left(\frac{i_2}{2^K}+\frac{1}{2^{K+1}}+\varepsilon_2\right)\,d\varepsilon_2\;d\varepsilon_1$$
$$=\frac{1}{2^{2K}}\left(1-\frac{2i_1+1}{2^{K+1}}\right)\frac{2i_2+1}{2^{K+1}},$$

and

$$\int_{-\frac{1}{2^{K+1}}}^{\frac{1}{2^{K+1}}}\int_{-\frac{1}{2^{K+1}}}^{\frac{1}{2^{K+1}}}\left\{1-\left[\frac{i}{2^K}+\frac{1}{2^{K+1}}+\max(\varepsilon_1,\varepsilon_2)\right]\right\}$$
$$\times\left[\frac{i}{2^K}+\frac{1}{2^{K+1}}+\min(\varepsilon_1,\varepsilon_2)\right]\,d\varepsilon_2\;d\varepsilon_1$$
$$=\int_{-\frac{1}{2^{K+1}}}^{\frac{1}{2^{K+1}}}\int_{-\frac{1}{2^{K+1}}}^{\varepsilon_1}\left[1-\left(\frac{i}{2^K}+\frac{1}{2^{K+1}}+\varepsilon_1\right)\right]$$
$$\times\left(\frac{i}{2^K}+\frac{1}{2^{K+1}}+\varepsilon_2\right)\,d\varepsilon_2\;d\varepsilon_1$$
$$+\int_{-\frac{1}{2^{K+1}}}^{\frac{1}{2^{K+1}}}\int_{\varepsilon_1}^{\frac{1}{2^{K+1}}}\left[1-\left(\frac{i}{2^K}+\frac{1}{2^{K+1}}+\varepsilon_2\right)\right]$$
$$\times\left(\frac{i}{2^K}+\frac{1}{2^{K+1}}+\varepsilon_1\right)\,d\varepsilon_2\;d\varepsilon_1$$
$$=\frac{3i+1}{3\cdot 2^{2K}}-\frac{4i^2+4i+1}{4\cdot 2^{3K}}.$$

This gives us

$$g_1(i_1,i_2,j_1,j_2)$$
$$=2^{K4^K}\int_{-\frac{1}{2^{K+1}}}^{\frac{1}{2^{K+1}}}\cdots\int_{-\frac{1}{2^{K+1}}}^{\frac{1}{2^{K+1}}}[1-\max(x_{2^K i_1+j_1},x_{2^K i_2+j_2})]$$
$$\times\min(x_{2^K i_1+j_1},x_{2^K i_2+j_2})\cdot[1-\max(y_{2^K i_1+j_1},y_{2^K i_2+j_2})]$$
$$\times\min(y_{2^K i_1+j_1},y_{2^K i_2+j_2})\;d\varepsilon_0\cdots d\varepsilon_{2^K-1}\;d\delta_0\;\ldots\;d\delta_{2^K-1}$$
$$=\left\{\begin{array}{ll}
\left(1-\frac{2i_1+1}{2^{K+1}}\right)\frac{2i_2+1}{2^{K+1}}\left(1-\frac{2j_1+1}{2^{K+1}}\right)\frac{2j_2+1}{2^{K+1}} & i_1>i_2,\,j_1>j_2\\
\left(1-\frac{2i_1+1}{2^{K+1}}\right)\frac{2i_2+1}{2^{K+1}}\left(1-\frac{2j_2+1}{2^{K+1}}\right)\frac{2j_1+1}{2^{K+1}} & i_1>i_2,\,j_1>j_2\\
\left(1-\frac{2i_1+1}{2^{K+1}}\right)\frac{2i_2+1}{2^{K+1}}\left(\frac{3j_1+1}{3\cdot 2^K}-\frac{4j_1^2+4j_1+1}{4\cdot 2^{2K}}\right) & i_1>i_2,\,j_1=j_2\\
\left(1-\frac{2i_2+1}{2^{K+1}}\right)\frac{2i_1+1}{2^{K+1}}\left(1-\frac{2j_1+1}{2^{K+1}}\right)\frac{2j_2+1}{2^{K+1}} & i_1<i_2,\,j_1>j_2\\
\left(1-\frac{2i_2+1}{2^{K+1}}\right)\frac{2i_1+1}{2^{K+1}}\left(1-\frac{2j_2+1}{2^{K+1}}\right)\frac{2j_1+1}{2^{K+1}} & i_1<i_2,\,j_1<j_2\\
\left(1-\frac{2i_2+1}{2^{K+1}}\right)\frac{2i_1+1}{2^{K+1}}\left(\frac{3j_1+1}{3\cdot 2^K}-\frac{4j_1^2+4j_1+1}{4\cdot 2^{2K}}\right) & i_1<i_2,\,j_1=j_2\\
\left(\frac{3i_1+1}{3\cdot 2^K}-\frac{4i_1^2+4i_1+1}{4\cdot 2^{2K}}\right)\left(1-\frac{2j_1+1}{2^{K+1}}\right)\frac{2j_2+1}{2^{K+1}} & i_1=i_2,\,j_1>j_2\\
\left(\frac{3i_1+1}{3\cdot 2^K}-\frac{4i_1^2+4i_1+1}{4\cdot 2^{2K}}\right)\left(1-\frac{2j_2+1}{2^{K+1}}\right)\frac{2j_1+1}{2^{K+1}} & i_1=i_2,\,j_1>j_2\\
\left(\frac{2i_1+1}{2\cdot 2^K}-\frac{3i_1^2+3i_1+1}{3\cdot 2^{2K}}\right)\left(\frac{2j_1+1}{2\cdot 2^K}-\frac{3j_1^2+3j_1+1}{3\cdot 2^{2K}}\right) & i_1=i_2,\,j_1=j_2
\end{array}\right\}.$$

Making more use of symmetry, the sum of these $g_1(i_1,i_2,j_1,j_2)$ is found to be

$$\begin{aligned}
&\sum_{i_1=0}^{2^K-1}\sum_{i_2=0}^{2^K-1}\sum_{j_1=0}^{2^K-1}\sum_{j_2=0}^{2^K-1} g_1(i_1,i_2,j_1,j_2)\\
&\quad=4\sum_{i_1=0}^{2^K-1}\sum_{i_2=0}^{i_1-1}\sum_{j_1=0}^{2^K-1}\sum_{j_2=0}^{j_1-1}\left(1-\frac{2i_1+1}{2^{K+1}}\right)\frac{2i_2+1}{2^{K+1}}\left(1-\frac{2j_1+1}{2^{K+1}}\right)\frac{2j_2+1}{2^{K+1}}\\
&\quad+4\sum_{i_1=0}^{2^K-1}\sum_{i_2=0}^{i_1-1}\sum_{j_1=0}^{2^K-1}\left(1-\frac{2i_1+1}{2^{K+1}}\right)\frac{2i_2+1}{2^{K+1}}\left(\frac{3j_1+1}{3\cdot 2^K}-\frac{4j_1^2+4j_1+1}{4\cdot 2^{2K}}\right)\\
&\quad+\sum_{i_1=0}^{2^K-1}\sum_{j_1=0}^{2^K-1}\left(\frac{2i_1+1}{2\cdot 2^K}-\frac{3i_1^2+3i_1+1}{3\cdot 2^{2K}}\right)\left(\frac{2j_1+1}{2\cdot 2^K}-\frac{3j_1^2+3j_1+1}{3\cdot 2^{2K}}\right)\\
&\quad=4\left(\frac{2^{4K}}{576}-\frac{2^{3K}}{144}+\frac{2^{2K}}{72}-\frac{5\cdot 2^K}{288}+\frac{1}{72}-\frac{1}{144\cdot 2^K}+\frac{1}{576\cdot 2^{2K}}\right)\\
&\quad+4\left(\frac{2^{3K}}{144}-\frac{2^{2K}}{48}+\frac{2^K}{32}-\frac{1}{36}+\frac{1}{72\cdot 2^{2K}}-\frac{1}{288\cdot 2^{2K}}\right)+\frac{2^{2K}}{36}\\
&\quad=\frac{2^{4K}}{144}+\frac{2^K}{36}-\frac{1}{18}+\frac{1}{36\cdot 2^K}-\frac{1}{144\cdot 2^{2K}}.
\end{aligned}$$

For the second summation, we use the result

$$\int_{-\frac{1}{2^{K+1}}}^{\frac{1}{2^{K+1}}}\left[1-\left(\frac{i}{2^K}+\frac{1}{2^{K+1}}+\varepsilon\right)\right]\left(\frac{i}{2^K}+\frac{1}{2^{K+1}}+\varepsilon\right)d\varepsilon=\frac{2i+1}{2\cdot 2^K}-\frac{3i^2+3i+1}{3\cdot 2^{3K}}$$

to get

$$\begin{aligned}
g_2(i_1,i_2,j_1,j_2)&=2^{K4^K}\int_{-\frac{1}{2^{K+1}}}^{\frac{1}{2^{K+1}}}\cdots\int_{-\frac{1}{2^{K+1}}}^{\frac{1}{2^{K+1}}}\left(1-x_{2^K i_1+j_1}\right)x_{2^K i_1+j_1}\\
&\quad\left(1-y_{2^K i_1+j_1}\right)\times y_{2^K i_1+j_1}\,d\varepsilon_0\ldots d\varepsilon_{2^K-1}\,d\delta_0\ldots d\delta_{2^K-1}\\
&=\left(\frac{2i+1}{2\cdot 2^K}-\frac{3i^2+3i+1}{3\cdot 2^{2K}}\right)\left(\frac{2j+1}{2\cdot 2^K}-\frac{3j^2+3j+1}{3\cdot 2^{2K}}\right).
\end{aligned}$$

The sum of the $g_2(i_1,i_2,j_1,j_2)$ is then

$$\begin{aligned}
\sum_{i=0}^{2^K-1}\sum_{j=0}^{2^K-1} g_2(i_1,i_2,j_1,j_2)&=\sum_{i=0}^{2^K-1}\sum_{j=0}^{2^K-1}\left(\frac{2i+1}{2\cdot 2^K}-\frac{3i^2+3i+1}{3\cdot 2^{2K}}\right)\\
&\quad\times\left(\frac{2j+1}{2\cdot 2^K}-\frac{3j^2+3j+1}{3\cdot 2^{2K}}\right)=\frac{2^{2K}}{36}.
\end{aligned}$$

Putting these together shows that the expected squared error of the T_N discrepancy for this sequence of points is

$$\begin{aligned}
&\frac{1}{2^{4K}}\left(\frac{2^{4K}}{144}+\frac{2^K}{36}-\frac{1}{18}+\frac{1}{36\cdot 2^K}-\frac{1}{144\cdot 2^{2K}}\right)-\frac{1}{2\cdot 2^{2K}}\left(\frac{2^{2K}}{36}\right)+\frac{1}{144}\\
&\quad=\frac{1}{18\cdot 2^{3K}}-\frac{1}{18\cdot 2^{4K}}+\frac{1}{36\cdot 2^{5K}}-\frac{1}{144\cdot 2^{6K}},
\end{aligned}$$

so

$$E(T_N)=\sqrt{\frac{1}{18N^{3/2}}-\frac{1}{18N^2}+\frac{1}{36N^{5/2}}-\frac{1}{144N^3}},$$

valid for N being an even power of 2. ■

REFERENCES

N. Bouleay and D. Lépingle, Numerical methods for stochastic processes, John Wiley, New York, 1994.

E. Braaten and G. Weller, An improved low-discrepancy sequence for multidimensional quasi-Monte Carlo integration, J Comput Phys 33 (1979), 249–258.

A.M. Bruckstein, R.J. Holt, and A.N. Netravali, Holographic representations of images, IEEE Trans Image Process 7 (1998), 1583–1597.

Y. Eldar, M. Lindenbaum, M. Porat, and Y.Y. Zeevi, The farthest point strategy for progressive image sampling, IEEE Trans Image Process 6 (1997), 1305–1315.

C. Gotsman and M. Lindenbaum, On the metric properties of discrete space-filling curves, IEEE Trans Image Process 5 (1996), 794–797.

J.H. Halton, A retrospective and prospective survey of the Monte Carlo method, SIAM Rev 12 (1970), 1–63.

J.H. Halton and S.K. Zaremba, The extreme and L^2 discrepancies of some plane sets, Monatshefte für Mathematik 73 (1969), 316–328.

L. Kocis and W.J. Whiten, Computational investigations of low-discrepancy sequences, ACM Trans Math Software 23 (1997), 266–294.

J. Lagarias, Well-spaced labelings of points in rectangular grids, SIAM J Discrete Math 13 (2000), 521–534.

G. Mitchison and R. Durbin, Optimal numberings of an $n \times n$ array, SIAM J Algebr Discrete Methods 7 (1986), 571–582.

W.J. Morokoff and R.E. Caflisch, Quasi-random sequences and their discrepancies, SIAM J Sci Comput 15 (1994), 1251–1279.

H. Niederreiter, "Random number generation and quasi-Monte Carlo methods," In CNBS-NSF Regional Conference Series in Applied Mathematics, Philadelphia, 1992, Vol. 63, pp. 161–176.

K.F. Roth, On irregularities of distribution, Mathematika 1 (1954), 73–79.

B. Tuffin, Improvement of Halton sequences distribution, Technical Report 998, Institut de Recherche en Informatique et Systèmes Aléatoires, Université de Rennes, March 1996.

I.V. Vilenkin, Plane nets of integration, USSR Comput Math Math Phys 7 (1967), 189–196.

T.T. Warnock, "Computational investigations of low-discrepancy point sets," Applications of number theory to numerical analysis, S.K. Zaremba (Editor), Academic Press, New York, 1972, pp. 319–333.

T.-T. Wong, W.-S. Luk, and P.-A. Heng, Sampling with Hammersley and Halton points, J Graph Tool 2 (1997), 9–24.

S.K. Zaremba, The mathematical basis of Monte Carlo and quasi-Monte Carlo methods, SIAM Rev 10 (1968), 303–314.